Nuclear Spin Analogues of Gyromagnetism: Case of the Zero–field Barnett Effect

E. L. Hahn[1], B. K. Tenn[2] and M. P. Augustine[2]

[1] Department of Physics, University of California, Berkeley, CA 94720
[2] Department of Chemistry, One Shields Avenue, University of California, Davis, CA 95616, augustin@chem.ucdavis.edu

1 Personal Tribute

I thank the editors for the invitation to write in honor of Robert Blinc and to celebrate his 70^{th} birthday. Over his many years of international research collaborations and leadership of NMR research groups at the Josef Stefan Institute, he and his colleagues have generated a body of comprehensive experimental data leading to new concepts and clarifications concerning unusual solid state structures. These have involved topics such as ferroelectrics, disordered systems, and liquid crystals, often connected with phase transitions and modal behavior.

While continually devoting himself to his group as a pioneering research physicist working out new interpretations of experiments, Professor Blinc also served as a leader of Slovenian science, maintaining many personal contacts as a virtual "Science Ambassador" in Europe. During the Cold War and through its waning years, because of Robert's international connections in the East, he was able to arrange contacts with people from both the East and the West to attend conferences in Slovenia and on the Dalmation Coast. He has made it possible for many NMR research people from the Eastern block to interact with those of us from the West. His international influence has been unique in making the world a better place for scientific cooperation. Personally I can testify how much we have enjoyed Robert's hospitality, friendship, and stimulation provided by visitations to interact with his NMR research group at the Josef Stefan Institute for which we are grateful. We wish him and his spouse many happy and fruitful years and that he should remain active and not really retire.

2 Introduction

The motivation of this work is the possibility of the ultra-sensitive detection of pico and femto-Tesla fields from the nuclear spin polarization induced in

spinning solids at zero field caused by the Barnett effect. Both the Superconducting Quantum Interference Device (SQUID) [1] and non-linear optical Faraday rotation methods [2] of measuring magnetic fields with an ultimate sensitivity of about one femto-Tesla $\mathrm{Hz}^{-1/2}$ or $10^{-11}\,\mathrm{G\,Hz}^{-1/2}$ promise to detect these small fields generated by diamagnetic solids.

A brief review of well known elementary principles of gyromagnetic experiments [3, 4] sets the stage for discussion of coupling mechanisms in the Barnett effect that may account for momentum transfer from a mechanically spinning macroscopic body to microscopic nuclear spins within the body. Only a minute fraction of the total mechanical angular momentum of the spinning sample is transferred to the oriented macroscopic magnetic spin angular momentum, thus conserving the total angular momentum of the system. In the absence of diamagnetic effects, the ratio of the change of the macroscopic magnetism of a rotating body to this corresponding change in angular momentum of the body is well known as the effective gyromagnetic ratio $(q/2mc)\ g$ where q is the fundamental charge, m is the electron mass, c is the speed of light, and g is the empirical g factor.

The Barnett effect was first observed in 1914 [4] by detecting the magnetism due to the polarization of electron spins caused by rotation of a cylinder of soft unmagnetized iron. Although the Barnett effect is looked upon today as an archaic experiment, it was an important experiment of the old physics era. Today many people are not aware of the Barnett effect because it is referred to so little in the literature. It is interesting that even though the concept of electron spin did not exist at that time, the original Barnett experiment provided the first evidence that the electron had an anomalous magnetic moment with a g factor of 2. Today it is well known that the electron spin g factor can also differ significantly from the value of 2 (ignoring the small radiative correction) because of spin orbit coupling. Barnett concluded in 1914 that he measured the gyromagnetic ratio of classical rotating charges q to be q/mc, an anomalous value twice the classical value he expected.

In 1915 Einstein and de Haas [5] carried out the converse of the Barnett experiment. The reversal of an initially known magnetization M_0, or the growth of M_0 from zero, of an iron cylinder produces a small mechanical rotation of the cylinder. In contrast to Barnett's experiment, there is an apparent transfer of spin angular momentum from M_0 into mechanical rotation. Curiously Einstein and de Haas reported $g = 1$ from their measurements, apparently rejecting data that deviated from the expected classical value of $g = 1$ to account for the orbital magnetism. In 1820 Ampere established that the current due to a charge q and mass m rotating in a circle of radius r, multiplied by circle area πr^2, expresses the classical orbital magnetic moment. This picture supported the idea of hidden classical Amperian currents in permanent magnets, a view that held sway into the early years of the 20^{th} century. But this view of classical magnetism, and ultimately the Einstein and de Haas $g = 1$ experimental interpretation, was first challenged by a theorem formulated by Miss van Leeuwen [6] and Bohr, namely, that any confined configuration of

free charges obeying classical laws of motion and precessing in any magnetic field must yield zero magnetic susceptibility. Finally the advent of momentum quantization and the concept of magnetic spin made possible a break away from the invalid classical picture of magnetism. The classical Amperian magnetic moment was replaced by the non-classical entity of magnetism, the Bohr magneton,

$$\mu = \frac{e\hbar}{2mc} = \gamma\hbar. \tag{1}$$

3 Parameter Rules for Interpretation of Gyromagnetic Experiments

Let the ratio $n\mu/n\hbar = M/\Omega = \gamma = e/2mc$ be defined from (1), where n is the number of polarized spins, or circulating charges in the old picture, lined up to define a macroscopic magnetic moment $M = n\mu$. The corresponding angular momentum is given by $\Omega = n\hbar$. By itself this ratio is a trivial identity, given that the Bohr magneton of every particle with $L = 1$ is $\mu = e\hbar/2mc$. The terms n and η contained in γ always cancel, implying in first order that the macroscopic body must display the same γ as a single spin would, and provide a measure of $e/2mc$ multiplied by any anomalous g factor. However this argument deserves a better physical justification, relating phenomenologically and still somewhat obscurely to the response of a gyroscope to torque. Sample rotation at a given frequency ω_r may be viewed as equivalent to a Larmor precession caused by a magnetic field H. As shown in Fig. 1, the imposed torque due to H tends to line up the spins. Changes in M and Ω evolve coaxially. They precess about H independent of the angle between H and M or Ω. A real magnetic field H causes spin precession of M about the direction of H while M develops and finally reaches equilibrium because of spin-lattice relaxation. However, if the sample is not left to rotate freely as in the Einstein-de Haas experiment, there can be no direct evidence of any mechanical exchange of momentum Ω no matter how minute. Except for certain special circumstances of macroscopic radiation damping, theories of spin relaxation keep track of energy degrees of freedom but not of elusive internal mechanisms of spin lattice momentum transfer.

Before the development of gyromagnetic experiments, in 1861 Maxwell perceived Amperian currents as hidden gyroscopic sources of permanent magnetism. He tried to detect the precession of a permanent magnet in response to an outside torque, but the effect is too small to detect. His attempt relates to Fig. 1. In place of a mechanical torque, the magnetic field H subjects the magnetization M to the torque $T = M \sin\theta\ H = \Omega \sin\theta\ \omega_r$. Including the empirical factor g the ratio

$$\frac{M}{\Omega} = \frac{\omega_r}{H} = \left(\frac{e}{2mc}\right) g \tag{2}$$

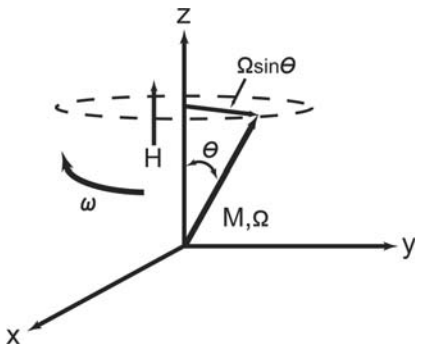

Fig. 1. Relationship of the magnetization M, rotational angular momentum Ω, and static magnetic field H used to discuss magnetomechanical rotation experiments.

defines values of M and Ω as final values representing changes from zero. As a gyromagnetic rule, M/Ω should be written as the ratio of changes $\Delta M/\Delta\Omega$ at any time in the evolution of the spin alignment. The Einstein-de Haas experiment measures the ratio of any imposed M change to the resulting sample rotation angular momentum which is observed. The Barnett experiment measures the ratio of ω_r to a calibrated H field that produces the same M caused by sample rotation at the frequency ω_r. Generation of a calibrated H in the pico to femto-Tesla range from a stable current source would be an extremely difficult requirement. No real field is present when the Barnett effect takes place. Instead, the field H in (2) acts like a "ghost" field H_{ghost}, having the same effect as a real field. Its definition relates to Larmor's theorem, where $H_{ghost} = \omega_r/\gamma$ is defined as an equivalent field. Equation (2) must follow from energy conservation arguments. A sample rotating at the rate ω_r and with moment of inertia I is endowed with rotational energy $U = I\omega_r^2/2$. Any small momentum transfer $\Delta\Omega = I\Delta\omega_r$ that might take place to the spins would require a corresponding increase in spin energy ΔMH. The total energy transferred between spin and rotation is then $\Delta U = I\omega_r\Delta\omega_r = \Delta\Omega\omega_r = \Delta MH$, a relation that immediately rearranges to express the gyroscopic rule given by (2).

4 Nuclear Spin Analogues

Prior to 1940, gyromagnetic experiments served as a measure of g values of electron spin systems in ferromagnetic and paramagnetic substances.[4] The Barnett magnetization, although at least a thousand times or more greater than nuclear spin magnetization in samples of comparable size, is very small, difficult to measure, and easily obscured by instrumental instabilities and stray fields. Even large magnetic fields in those days could not be measured to better than a fraction of a percent by rotating pick up coils. These methods

are now obsolete, superseded by the application of magnetic resonance detection methods.[7, 8, 9] As a physical mechanism, the nuclear Barnett effect was invoked later by Purcell [10] to account for the observation of weakly polarized starlight. In that account, Purcell discusses the mechanism of differential light scattering from fast "suprathermal" rotating grains in interstellar space. Because of their rotation it is postulated that these grains become magnetized due to the nuclear Barnett effect. The common directivity and polarization of light scattering by the grains occurs over vast distances because the polarized grains in turn precess about the direction of weak interstellar magnetic fields.

Rather than discuss parameters of this very special unearthly case [11] of Barnett polarization, consider a more representative and yet marginal case on Earth. Here a $1\,\mathrm{cm}^3$ sample of $N = 10^{22}$ nuclear Bohr magnetons where $\mu_B = (9.27/1840) \times 10^{-21}\,\mathrm{erg\,G^{-1}}$ is rotated at the rate $\omega_r/2\pi = 4\,\mathrm{kHz}$ in zero applied magnetic field at $T = 300\,\mathrm{K}$. Assume that the sample acquires an equilibrium magnetization $M_0 = N\mu_B(\hbar\omega_r/kT)$ because of spin lattice relaxation in the ghost field $H_{ghost} = \omega_r/\gamma$. The resulting polarization field in the sample is about $4\pi M_0 \approx 10^{-10}$ G or about 1–10 femto-Tesla. Clearly rotation at higher speeds and at lower temperature could provide M_0 values 10 to 100 times larger, providing an extra margin for weak field detection.[1, 2]

5 Homonuclear Dipole-Dipole Coupling

The crude estimate of the field due to a Barnett induced magnetization mentioned above assumes that the spins polarize in a ghost field $H_{ghost} = \omega_r/\gamma$ during a spin-lattice relaxation process as though it were a real field. However, the complexity of many momentum transfer relaxation mechanisms between spin and lattice thermal reservoirs is too difficult to handle. Some understanding can be gained from a specific example of momentum conservation by simulating the effect of sample spinning on dipolar interactions among nuclear spins. A rigid lattice firmament of spins is assigned only a spin temperature with lattice coordinates θ, r and ϕ independent of time in the absence of sample spinning. Since there is no lattice thermal reservoir in this picture, the source of magnetization is obtained from previously prepared dipolar order in zero field that is converted to magnetization by sample rotation. A simple starting point considers two identical spins I_1 and I_2 separated by the distance r and coupled via their dipolar fields. A real DC magnetic field H_0, or sample spinning at the rate ω_r may be applied separately or simultaneously, axially or non-axially. The dipolar coupling is defined as $\mathcal{H}_D = \omega_D \sum (-1)^q T_q^{(2)}(I_1, I_2) R_{-q}^{(2)}(\theta, \phi)$ where $\omega_D = \gamma_1\gamma_2\hbar/r^3$ and the irreducible components $T_q^{(2)}(I_1, I_2)$ and $R_q^{(2)}(\theta, \phi)$ are given by

$$\begin{aligned} T^{(2)}_0(I_1,I_2) &= \tfrac{1}{\sqrt{6}}(3I_{z,1}I_{z,2} - I_1 g I_2) & R^{(2)}_0(\theta,\phi) &= \tfrac{\sqrt{6}}{2}(1-3\cos^2\theta), \\ T^{(2)}_{\pm 1}(I_1,I_2) &= \tfrac{1}{\sqrt{2}}(I_{\pm,1}I_{z,2} + I_{z,1}I_{\pm,2}) & R^{(2)}_{\pm 1}(\theta,\phi) &= \pm 3\sin\theta\cos\theta \mathrm{e}^{\pm \mathrm{i}\phi}, \\ T^{(2)}_{\pm 2}(I_1,I_2) &= I_{\pm,1}I_{\pm,2} & R^{(2)}_{\pm 2}(\theta,\phi) &= \tfrac{3}{2}\sin^2\theta \mathrm{e}^{\pm 2\mathrm{i}\phi}. \end{aligned} \quad (3)$$

When written in this way it should be clear that $\mathcal{H}_D$ not only couples the spins I_1 and I_2 to each other with the $T^{(2)}_q(I_1,I_2)$ operators, but also to the lattice with the $R^{(2)}_q(\theta,\phi)$ coefficients. The lattice degrees of freedom with large heat capacity are usually assumed to be at constant temperature in diagonal states of the density matrix, while the spin temperature may change due to relaxation. For this reason the understanding of NMR experiments in solids considers only the effect of the lattice on the spins, while effects of the spins on the lattice are usually neglected. However gyromagnetic experiments confirm that the lattice hooked to the rotor does exchange angular momentum with the spins, showing that the spins have a momentum effect on the lattice. In connection with nuclear spin diffusion in zero field, Sodickson and Waugh [12] introduced the interesting and related question about momentum exchange and conservation between nuclear spins and the lattice in zero field. Here the components of the angular momentum operators $\boldsymbol{L} = \boldsymbol{r} \times \boldsymbol{p}$ are given by

$$\begin{aligned} L_x &= \mathrm{i}(\sin\phi\frac{\partial}{\partial\theta} + \cot\theta\cos\phi\frac{\partial}{\partial\phi}), \\ L_y &= \mathrm{i}(-\cos\phi\frac{\partial}{\partial\theta} + \cot\theta\sin\phi\frac{\partial}{\partial\phi}), \\ L_z &= -\mathrm{i}\frac{\partial}{\partial\phi}, \end{aligned} \quad (4)$$

which in combination with Ehrenfest's theorem can be used to show that the time derivative of the expectation value of the total spin angular momentum $\boldsymbol{J} = \boldsymbol{I}_1 + \boldsymbol{I}_2$ is given by

$$\frac{\mathrm{d}}{\mathrm{d}t}\langle \boldsymbol{J}\rangle = \langle \boldsymbol{I}_1 \times \boldsymbol{H}_{D,2}\rangle + \langle \boldsymbol{I}_2 \times \boldsymbol{H}_{D,1}\rangle = \mathrm{i}\langle[\mathcal{H}_D, \boldsymbol{J}]\rangle = -\frac{\mathrm{d}}{\mathrm{d}t}\langle \boldsymbol{L}\rangle, \quad (5)$$

where $\boldsymbol{H}_{D,1}$ and $\boldsymbol{H}_{D,2}$ are the dipolar fields from spin 1 and 2. This reformulation of Bloch's equation shows that the total angular momentum, spin plus lattice, is conserved. This angular momentum conservation relationship is at the heart of recovering Zeeman order from dipolar order by sample rotation and can be used to determine the effect of the spins on the lattice. As an example consider an ensemble of identical dipole-dipole coupled two spin systems at thermal equilibrium in zero applied magnetic field. The thermal equilibrium density operator corresponding to this situation is given by $\rho_{eq} = \exp(-\mathcal{H}_D/kT) \approx 1 - \mathcal{H}_D/kT$ where k is the Boltzmann constant and the high temperature approximation has been applied. Provided that there are no real magnetic fields present, the expectation value $\langle \boldsymbol{J}\rangle = Tr\{\rho_{eq}\ \boldsymbol{J}\}$

is zero at all times. In order to verify (5) or equivalently show that $\langle \boldsymbol{L} \rangle = 0$ in this example, a rigorous quantum mechanical treatment of the expectation value of the lattice angular momentum $\langle \boldsymbol{L} \rangle$ is needed. This treatment requires that the rotational motion of the lattice be quantized in direct analogy to the rotational level structure in molecular H_2 gas [7] or in tunneling methyl groups [13]. Adopting this approach requires some knowledge of the partition function corresponding to rotation in addition to the calculation of the matrix elements of the $R_q^{(2)}(\theta, \phi)$ coefficients from the $|L, m\rangle = Y_m^{(L)}(\theta, \phi)$ spherical harmonic basis functions. In the case of H_2 gas in a molecular beam where the moment of inertia I is small, molecular rotation is fast, and the temperature is low, it is safe to truncate the basis set to a finite number of rotational energy levels. However, in the case of a real macroscopic sample at room temperature, I is large and the sample rotation is slow. This means that an untractably large number of very closely spaced energy levels will be populated at thermal equilibrium. The inability to define the density matrix of the rotor in this case can be circumvented by realizing that the expectation value for the lattice angular momentum $\langle \boldsymbol{L} \rangle$ must reduce to the classical result $I\omega_r$ for a macroscopic object. In this way in zero field (5) reduces to

$$\frac{\mathrm{d}}{\mathrm{d}t}(I\omega_r) = -\frac{\mathrm{d}}{\mathrm{d}t}\langle \boldsymbol{J} \rangle, \tag{6}$$

therefore in the absence of sample rotation, $\omega_r = 0$ and $\langle \mathbf{L} \rangle = \mathrm{I}\omega_r = 0$.

Equation (6) contains a very important result, namely, any change in sample rotation rate ω_r will lead to a corresponding change in sample magnetization. If a stationary sample is initially in zero magnetic field, (6) indicates that a jump in rotational frequency from zero to a final value ω_r will lead to a corresponding change in sample magnetization from zero to a final value. In certain special cases like the ensemble of identical two spin systems mentioned above, (6) can be used in combination with the solution to the Liouville-von Neumann equation during sample spinning along the $+z$ direction to determine the dynamics of both the formation of magnetization $\langle \boldsymbol{J} \rangle$ and the change in the spin rate ω_r due to this magnetization. Here the static dipolar coupling $\mathcal{H}_D$ mentioned above becomes time dependent in $\phi(t)$ as $\mathcal{H}_D(t) = \omega_D \sum (-1)^q T_q^{(2)}(I_1, I_2) R_{-q}^{(2)}(\theta, \phi) \mathrm{e}^{\mathrm{i}q\omega_r t}$ since the internuclear vector $\boldsymbol{r}$ now precesses about the rotation direction taken along $+z$. This particular time dependent form for the laboratory frame Hamiltonian $\mathcal{H}_{lab} = \mathcal{H}_D(t)$ is not convenient for practical calculations and does not offer much insight into how magnetization develops due to sample spinning. The symmetry between the $T_q^{(2)}(I_1, I_2)$ and $R_q^{(2)}(\theta, \phi)$ products in $\mathcal{H}_D(t)$ permit the $\exp(\mathrm{i}q\omega_r t)$ time dependence to be grouped together with the spin operators as $T_q^{(2)}(I_1, I_2) \exp(\mathrm{i}q\omega_r t)$ instead of with the $R_q^{(2)}(\theta, \phi)$ spatial terms that describe the orientation of $\boldsymbol{r}$ as a function of time. In this way it is clear that transformation to a rotating frame in spin space by rotation operator $U(\omega_r t) = \mathrm{e}^{\mathrm{i}qI_z\omega_r t}$ about the laboratory $+z$ axis as

$U(\omega_r t)\ T_q^{(2)}(I_1, I_2)\ U^\dagger(\omega_r t) = T_q^{(2)}(I_1, I_2) \exp(\mathrm{i}q\omega_r t)$ yields the time independent rotating frame Hamiltonian

$$\mathcal{H}_{rot} = \omega_r(I_{z,1} + I_{z,2}) + \omega_D \sum (-1)^q T_q^{(2)}(I_1, I_2) R_{-q}^{(2)}(\theta, \phi), \tag{7}$$

where the ghost field $H_{ghost} = \omega_r/\gamma$ appears. As expectation values of the total spin magnetization $\langle \boldsymbol{J} \rangle$ are independent of unitary transformations in the trace, the fictitious term in the rotating frame generates the same magnetization that a real field $H_0 = H_{ghost}$ would develop in the laboratory frame. Furthermore, since (5) and (6) relate traces of spin and lattice momentum operators, these relations are also frame independent.

A combination of the solution to the Liouville-von Neumann equation in the rotating frame using $\mathcal{H}_{rot}$ in (7) with the angular momentum conservation rule in (6) allows the dynamics of the magnetization and the rotor frequency to be determined starting from a stationary sample in zero magnetic field. Figure 2 shows the effect of instantaneously switching on an $\omega_r/2\pi = 10\,\mathrm{kHz}$ sample rotation to an ensemble of dipolar coupled two spin systems with $\omega_D/2\pi = 10\,\mathrm{kHz}$. The plots in Fig. 2(a) are appropriate for an ensemble of identical two-spin systems with $\theta = \pi/2$ and $\phi = 0$ while the plots in Fig. 2(b) describe a somewhat more realistic case involving an isotropic distribution of θ and ϕ values. In both of these plots the feedback due to angular momentum conservation requires that the alternating magnetization will modulate the $\omega_r/2\pi = 10\,\mathrm{kHz}$ applied sample spin rate. In addition the phase of the periodicity introduced into the spin rate is 180° out of phase with the periodicity in $\langle J_z \rangle$, consistent with the negative sign in (6). The same two spin system used in Fig. 2(a) was used to determine the peak z magnetization as a function of applied rotation rate in Fig. 2(c). This plot demonstrates that the largest Barnett magnetization can be obtained in zero field when $\omega_r \approx \omega_D$.

It is natural to ask if an analogue of the above experiments can be obtained by causing an ensemble of two-spin systems at thermal equilibrium in zero field to rotate by instantaneously jumping a real DC magnetic field. Introduction of a real DC magnetic field H_0 along the $+z$ direction in the laboratory frame where $\theta = 0$ adds a Zeeman term $\mathcal{H}_z = \gamma H_0(I_{z,1} + I_{z,2})$ to the dipolar coupling Hamiltonian $\mathcal{H}_D$ yielding the full laboratory frame Hamiltonian as $\mathcal{H}_{lab} = \mathcal{H}_z + \mathcal{H}_D$. One consequence of the field H_0 is to add an additional term to the zero field angular momentum conservation relation shown in (5) since $\mathrm{d}\langle \boldsymbol{L} \rangle/\mathrm{d}t = \mathrm{i}\langle [\mathcal{H}_{lab}, \boldsymbol{L}] \rangle = \mathrm{i}\langle [\mathcal{H}_D, \boldsymbol{L}] \rangle = -\mathrm{i}\langle [\mathcal{H}_D, \boldsymbol{J}] \rangle$ and $\mathrm{d}\langle \boldsymbol{J} \rangle/\mathrm{d}t = \mathrm{i}\langle [\mathcal{H}_{lab}, \boldsymbol{J}] \rangle = \mathrm{i}\langle [\mathcal{H}_z, \boldsymbol{J}] \rangle + \mathrm{i}\langle [\mathcal{H}_D, \boldsymbol{J}] \rangle$. Rearranging these equations, noting that $\langle \boldsymbol{L} \rangle$ commutes with $\mathcal{H}_z$, and using the fact that $\langle \boldsymbol{L} \rangle = I\omega_r$ in the classical limit recasts (5) as

$$\frac{\mathrm{d}}{\mathrm{d}t}(I\omega_r) = -\frac{\mathrm{d}}{\mathrm{d}t}\langle \boldsymbol{J} \rangle + \mathrm{i}\,\langle [\mathcal{H}_z, \boldsymbol{J}] \rangle = -\mathrm{i}\,[\mathcal{H}_D, \boldsymbol{J}]\,. \tag{8}$$

The expectation values are the same regardless of reference frame since the trace is independent of unitary transformation. Comparison of (8) to (6) shows

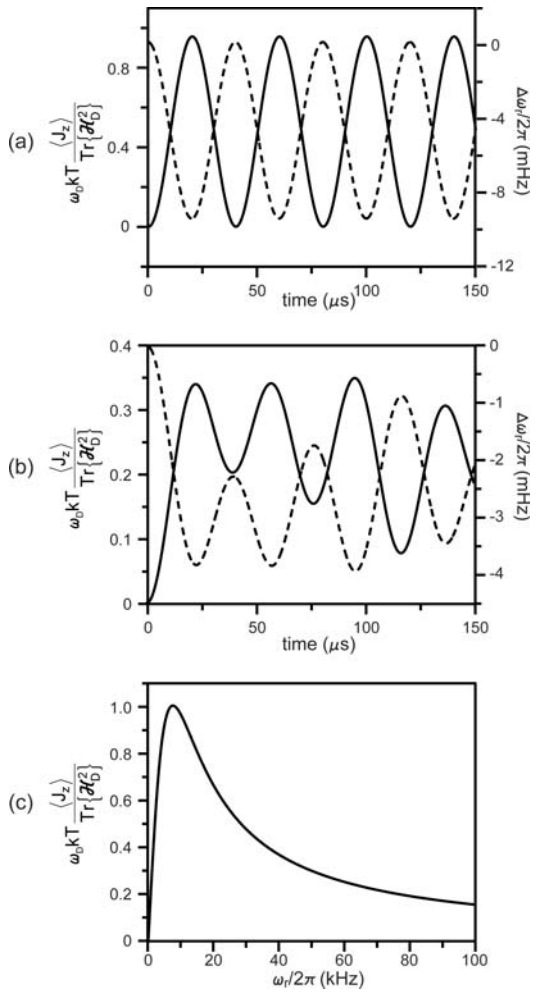

Fig. 2. Simulation of the dynamics of the two spin system rotating at the frequency $\omega_r/2\pi$ with $\omega_D/2\pi = 10\,\mathrm{kHz}$ and $\omega_0/2\pi = 0$. In each case (a)–(c) the $t < 0$ thermal equilibrium condition corresponds to an ensemble of two spin systems in zero magnetic field. At the time $t = 0$ the spin rate is instantaneously increased from zero to $\omega_r/2\pi = 10\,\mathrm{kHz}$ in (a) and (b) and a variable level in (c). The effects of the sample rotation are to create magnetization (solid line) as shown by the left ordinate in (a) and (b) for the $\theta = \pi/2$ orientation and the isotropic powder respectively. The polarization $\langle J_z \rangle = \langle I_{z,1} + I_{z,2} \rangle$ is scaled by the initial density operator so that a left ordinate value of 1 corresponds to a polarization of $\hbar\omega_D/2kT$. The right ordinate shows how the magnetization feeds back via angular momentum conservation to provide only mHz changes in the spin rate (dashed line) because the ratio $N\hbar/I$ is only $10^{-3}\,\mathrm{s}^{-1}$ for a real sample containing N spins. The plot in (c) suggests that the maximum transfer of rotational angular momentum into Zeeman polarization occurs when $\omega_r = \omega_D$.

that the interaction of the spin angular momentum $\boldsymbol{J}$ with the applied DC field H_0 represents an additional source of angular momentum that indirectly influences the momentum conservation. The rotor only exchanges angular momentum with the spins through $\mathcal{H}_D$, the dipolar interaction – not through the direct coupling with $\mathcal{H}_z$. The external $\mathcal{H}_z$ or any other applied field represents an energy-momentum source from a solenoid or an oscillator not directly coupled to the rotor. When initial angular momentum flows into J_z by jumping the rotation frequency from zero to ω_r, the built in feedback in (6) and demonstrated by simulation in Fig. 2 gives rise to the ghost field $H_{ghost} = \omega_r/\gamma$. This field can not couple to the solenoid. On the other hand, when an applied field is jumped from zero to H_0 the source of angular momentum flowing into J_z is the solenoid. The solenoid plays the role now of the rotor because of the application of an electromotive force which launches a current and therefore momentum into the applied H_0 field. The resulting exchange of order between the dipolar and Zeeman reservoirs is that of the Strombotne and Hahn experiment.[14] Therefore, $\mathcal{H}_z$ has only an indirect effect on the rotor but remains to define the Zeeman Bloch equations when $\omega_r = 0$. Equation (8) also explains why neither the Barnett nor the Einstein-de Haas effects have been noticed in routine NMR experiments in solids performed at high field. At high magnetic field the nuclear Zeeman interaction scales the non-secular $q \neq 0$ part of the dipole-dipole coupling to roughly $\omega_D^2/\omega_0 \ll \omega_D \ll \omega_0$. To zeroth order in perturbation theory the NMR spectrum is governed by the Zeeman interaction $\mathcal{H}_z$ and the right hand side of (8) is identically zero thus removing any coupling between the nuclear spin and mechanical angular momenta. Extending this argument to first order in perturbation theory also does not yield any useful coupling between ω_r and $\langle \boldsymbol{J} \rangle$ when the applied DC field is parallel to the sample spinning axis because the spatial term $T_0^{(2)}(I_1, I_2)R_0^{(2)}(\theta, \phi)$ does not have any ω_r rotational dependence. It is the time dependence imparted on the $q \neq 0$ parts of $\mathcal{H}_D(t)$ that translate into the generation of magnetization in zero magnetic field or the onset of sample rotation in a magnetic field. This can be appreciated by considering the Hamiltonian for the two-spin system with a magnetic field applied parallel to the sample spinning axis along the $+z$ direction. This time dependent Hamiltonian $\mathcal{H}_{lab} = \mathcal{H}_z + \mathcal{H}_D(t)$ is best considered in the rotating frame at the frequency ω_r. Since this transformation involves a rotation about the z axis, the nuclear Zeeman interaction $\mathcal{H}_z$ is simply added to the Hamiltonian in (7) to give

$$\mathcal{H}_{rot} = (\omega_r + \omega_0)(I_{z,1} + I_{z,2}) + \omega_D \sum (-1)^q T_q^{(2)}(I_1, I_2)R_{-q}^{(2)}(\theta, \phi), \qquad (9)$$

a result suggesting that sample rotation can either add to or subtract from the apparent Larmor frequency ω_0. Judging from (9) the largest effect of magnetic field on sample rotation would be in low-field where ω_r is comparable to ω_0, and given (8) combined with the zero field results mentioned above, the largest effect should be observed when ω_r is comparable to ω_D.

In direct analogy to the zero field case mentioned in Fig. 2, a combination of the solution to the Liouville-von Neumann equation in the rotating frame using $\mathcal{H}_{rot}$ in (9) with the angular momentum conservation rule in (8) permits the dynamics of the magnetization and the rotor frequency to be determined starting from a stationary sample in zero magnetic field. Figure 3 demonstrates the effect of instantaneously switching on an $H_0 = 2.35\,\mathrm{G}$ DC magnetic field or equivalently an $\omega_0/2\pi = 10\,\mathrm{kHz}$ ^{1}H Larmor frequency to an ensemble of dipole-dipole coupled two spin systems with $\omega_D/\pi = 10\,\mathrm{kHz}$. The plots in Fig. 3(a) correspond to the same ensemble of identical two-spin systems with $\theta = \pi/2$ and $\phi = 0$ shown in Fig. 2(a) while the plots in Fig. 3(b) show results for the same isotropic distribution of θ and ϕ values used in Fig. 2(b). In both of these plots the feedback due to angular momentum conservation requires that the magnetization will generate a periodic sample rotation. Since the commutator in (8) is always zero for the case of a field applied parallel to the maximum moment of inertia, the negative sign in (8) causes the phase of the periodicity in the spin rate to be 180° out of phase with the periodicity in $\langle J_z \rangle$. The same two-spin system used in Fig. 3(a) was used to determine the peak spin rate ω_r as a function of applied DC field and hence Larmor frequency ω_0 in Fig. 3(c). This plot demonstrates that the largest induced sample rotation rate starting in zero field can be obtained when the applied magnetic field H_0 is comparable to the inherent dipolar field i.e. when $H_0 \approx \omega_D/\gamma$ or $\omega_0 \approx \omega_D$.

The effects predicted by the admittedly crude two-spin system in Figs. 2 and 3 continue to manifest themselves in larger more realistic cases [14]. Figure 4 shows the Barnett initially induced magnetization in (a) and the DC field jump induced rotation in (b) for an eight spin system. In these examples the eight spins are positioned on the corners of a stationary cube in zero magnetic field that occupies the normal x, y, and z cartesian axis system while the gated sample rotation and magnetic field directions are along the $+z$ axis. The side length of the cube is 2.3 Å giving an $\omega_D/2\pi = 10\,\mathrm{kHz}$ dipolar coupling for protons with the smallest separation. In this example thermal equilibrium is appropriate for an ensemble of identical eight spin cubes held at the temperature T. To remain consistent with Figs. 2 and 3, the rotation speed in Fig. 4(a) is jumped from zero to $\omega_r/2\pi = 10\,\mathrm{kHz}$ while the field is jumped from zero to $H_0 = \omega_0/2\pi\gamma = 2.35\,\mathrm{G}$ in Fig. 4(b). Comparison of Fig. 4 to Figs. 2 and 3 suggest that the dynamics of the eight spin system are similar to that for the two spin system. The major difference is that the presence of three different dipolar coupling values corresponding to spins separated on the edge, face diagonal, and body diagonal of the cube, have the net effect of smearing the Zeeman-dipolar oscillations in Figs. 2 and 3, an averaging that makes the eight spin simulation closely resemble oscillations observed in real field cycled experiments.[14] Admittedly, Figs. 2(a) and 3(a), Figs. 2(b) and 3(b), Figs. 2(c) and 3(c), and Fig. 4(a) and Fig. 4(b) look identical. This similarity is intended as the ghost field due to sample rotation in Figs. 2 and 4(a) yield the same dynamics by independent calculations as the real field in Figs. 3 and 4(b). In Figs. 2–4 one may interpret in the case of jumping

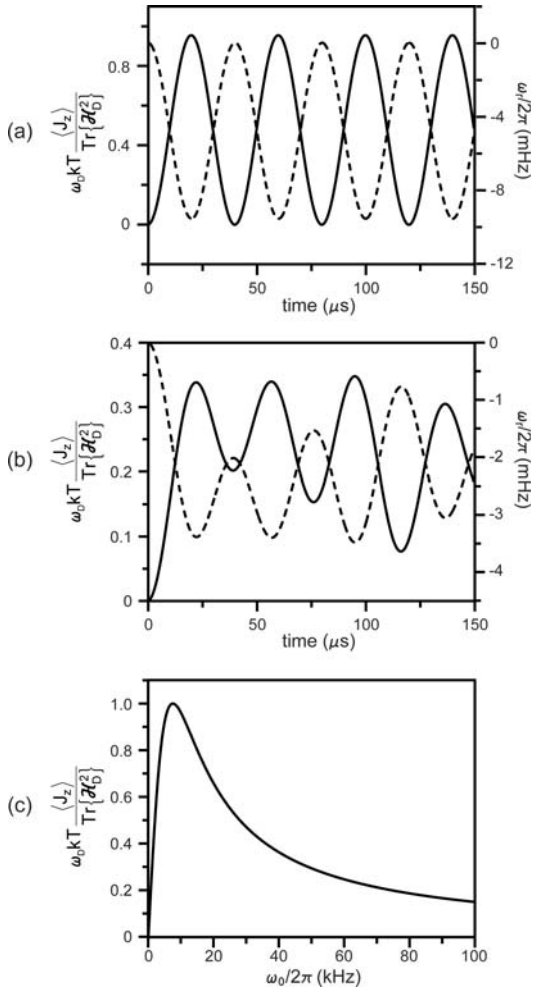

Fig. 3. Simulation of the dynamics of the two spin system with applied DC field at frequency $\omega_0/2\pi$ with $\omega_D/2\pi = 10\,\mathrm{kHz}$ and $\omega_r/2\pi = 0$. In each case (a)–(c) the $t < 0$ thermal equilibrium condition corresponds to an ensemble of two spin systems in zero magnetic field. At the time $t = 0$ the DC magnetic field is instantaneously increased from zero to $\gamma H_0 = \omega_0/2\pi = 10\,\mathrm{kHz}$ in (a) and (b) and a variable level in (c). The effects of this field are to create magnetization (solid line) as shown by the left ordinate in (a) and (b) for the $\theta = \pi/2$ orientation and the isotropic powder respectively. The polarization $\langle J_z \rangle$ is scaled by the initial density operator so that a left ordinate value corresponds to a polarization of $\hbar\omega_D/2kT$. The right ordinate shows how the magnetization feeds back via angular momentum conservation to provide mHz values for the spin rate (dashed line) because the ratio $N\hbar/I$ is only $10^{-3}\,\mathrm{s}^{-1}$ for a real sample containing N spins. The plot in (c) suggests that the maximum production of Zeeman polarization occurs when $\omega_0 = \omega_D$.

the rotor frequency from zero to ω_r, that when momentum flows from J_z to the rotor, the process is Einstein-de Haas. If the momentum flows from the rotor to J_z the process is Barnett. Hence there is an oscillatory display of both effects. These oscillations due to angular momentum conservation can be connected with the oscillations in energy due to population exchange between Zeeman and dipolar order.

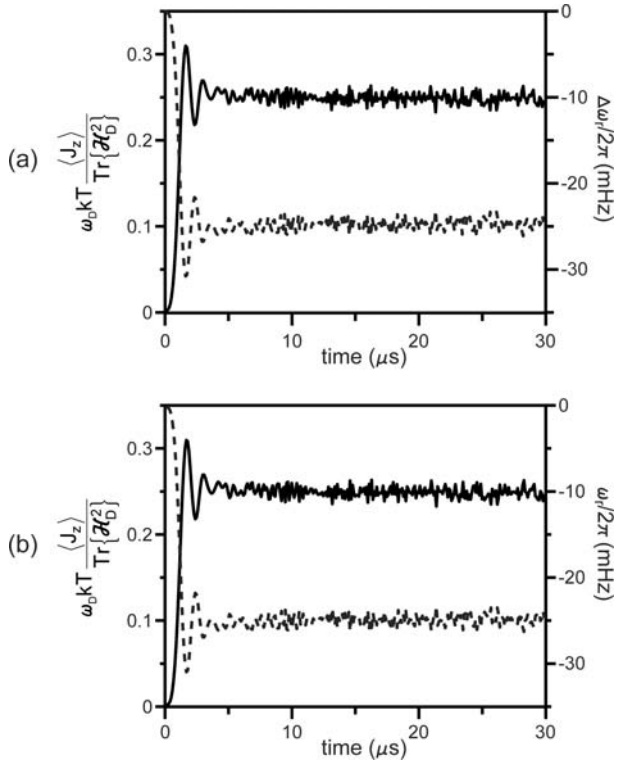

Fig. 4. Simulation of the dynamics of an eight spin system with the spins centered on the corners of a cube. Taking the spins as protons, the $\omega_D/2\pi = 10\,\mathrm{kHz}$ dipolar coupling corresponds to the strongest coupling or the shortest distance between nuclei on the 2.3 Å long cube side. The plot in (a) corresponds to jumping of an $\omega_r/2\pi = 10\,\mathrm{kHz}$ sample rotation rate while in (b) similar results are explored by turning on an $\omega_0/2\pi = 10\,\mathrm{kHz}$ Larmor frequency. In both cases the $t < 0$ thermal equilibrium situation reflects an ensemble of dipolar coupled eight spin systems. Here the value of the magnetization on the left ordinate is scaled to the thermal equilibrium density operator for the eight spin system while the right ordinate pertains to changes in the sample rotation frequency due to angular momentum conservation.

6 Adiabatic Demagnetization and Remagnetization

Because of spin entropy conservation in a homonuclear dipolar coupled spin system [15, 16] in the absence of relaxation, the adiabatic demagnetization of a spin system converts Zeeman order to dipolar order after an initial polarizing Zeeman field H_i is reduced adiabatically to zero. During this process, the initial spin temperature is reduced from T_i to a final dipolar spin temperature $T_f = (H_{loc}/H_i)\ T_i$ assuming $H_i \gg H_{loc}$, where $H_{loc} \propto \omega_D/2\pi\gamma$ is the local average dipolar field. Suppose that the thermodynamic relation $\mathrm{d}U = -M\mathrm{d}H$ governing the adiabatic process of demagnetization in the presence of a real field H applies also to the ghost field H_{ghost}. More accurately, this means that the spin temperature will be a function of the ghost field H_{ghost} as if it were a real field. On this basis any polarization induced by sample spinning will be Barnett in character. When a real field H_i is reduced during demagnetization, the adiabatic reduction in Zeeman energy $-M\Delta H$ requires that the spins must do work on the solenoid. Conversely the solenoid must do work on the spins to restore $M\Delta H$ in the process of remagnetization. With the case of a Barnett polarization mediated by sample spinning, it is necessary to show experimentally that the ghost field H_{ghost} can bring about an analagous adiabatic response. This would seem to follow by virtue of the identity $dU = -(M/\gamma)(\gamma \mathrm{d}H_{ghost}) = -\Omega \mathrm{d}\omega_r$, if in this case positive and negative work must be done by the rotor instead of the solenoid. If this picture is true, the outside work by the rotor must be different and not related to the microscopic changes in rotor energy and momentum mentioned in connection with spin lattice relaxation. There is an ambiguity here because the same terms that apply to either situation have been invoked by assuming that the same spin temperature applies in both cases. A negative or positive H_{ghost} added parallel to H by sample spinning in opposite directions would require both of these mechanisms to operate simultaneously.

In the limit that the ghost field behaves just like a real field, a sizeable portion of initially polarized magnetization $M_i = C_{spin}H_i/T_i$ may be recovered and sustained after adiabatic demagnetization by turning on a small ghost field H_{ghost}. Here the initial field H_i is sizeable and C_{spin} is the nuclear spin Curie constant. After adiabatic remagnetization in the ghost field H_{ghost}, a good fraction of M_i given by

$$M_f = M_i \frac{H_{ghost}}{\sqrt{H_{ghost}^2 + \langle H_{loc}^2 \rangle}} = M_i \frac{\omega_r}{\sqrt{\omega_r^2 + \langle \omega_D^2 \rangle}} \tag{10}$$

should be recovered due to the sample spinning. Since the adiabatically recovered magnetization in (10) is not directly proportional to H_{ghost} or equivalently ω_r as it is in the genuine Barnett effect, the final magnetization M_f should be considered as a re-magnetized "pseudo–Barnett" polarization suspended in the absence of real fields. Beginning at room temperature with-

out demagnetization one would obtain a much smaller magnetization $M_i = C_{spin}H_{ghost}/T_i$.

The dynamics of the "pseudo-Barnett" polarization in a small ghost field can be easily tested using the ensemble of eight spin systems described above. Here the initial thermal equilibrium polarization is taken to be in the high field high temperature limit $\rho_{eq} = 1 - \mathcal{H}_z/kT - \mathcal{H}_D/kT$ where both the Zeeman $\mathcal{H}_z$ and dipolar coupling $\mathcal{H}_D$ Hamiltonians are appropriate for eight spins situated at the corners of a cube. The Zeeman and dipolar temperatures are taken to be the same, and the field H_i is parallel to the sample spinning direction in addition to defining the $+z$ axis. Figure 5(a) shows the timing of the real magnetic field and sample rotation ramps during the adiabatic demagnetization and remagnetization process while Figs. 5(b)–(d) show how the total magnetization $\langle J_z \rangle$, dipolar order $\langle \mathcal{H}_D \rangle$, and spin rate ω_r evolve in time respectively. Comparison of Figs. 5(b) and (c) indicate that the demagnetization process from a field of $H_i = 2,350\,\mathrm{G}$ to zero completely transfers proton Zeeman order into dipolar order at the end of the ramp at $t = 100\,\mu\mathrm{s}$. After persisting as dipolar order for $t = 250\,\mu\mathrm{s}$, the adiabatically ramped sample spinning from zero to a final value of $\omega_r/2\pi = 30\,\mathrm{kHz}$ causes the "pseudo-Barnett" magnetization to appear. The dashed line in Fig. 5(b) corresponds to the ratio M_f/M_i anticipated on the basis of (10) with $\omega_r/2\pi = 30\,\mathrm{kHz}$ and $\langle \omega_D^2 \rangle^{1/2} = 16\,\mathrm{kHz}$ for the eight spin problem. Figures 5(b)–(d) all display what appears to be a large amount of noise at low field. Closer inspection of these plots reveals that the noise is periodic and that the source of the periodicity is the angular momentum feedback due to the Barnett effect.

7 Sample Spinning Non-axial with DC Field

In all of the previous cases with the DC field and sample rotation applied in the $+z$ direction, $\langle J_x \rangle = \langle J_y \rangle = 0$ and any feedback contributions due to off axis sample rotation are discarded in (6) and (8). The more useful case applying to narrow NMR lines in solids involves rapid sample spinning at some angle with respect to an applied DC field. New time dependent terms in the Hamiltonian are generated from rotation transformations of only the secular terms. In a small magnetic field comparable to the dipolar field, inclusion of the transformation of the non-secular terms show that any static field component normal to the axis of spin rotation results in saturation of any polarization M_0 that may be acquired by the Barnett effect. The coupling of the sample spinning to the magnetization in the case when a real DC field is applied at some initial angle that is not parallel to the direction of sample rotation can be understood by writing the dipolar coupling interaction in the principal axis frame of the moment of inertia tensor I. In this frame the z-axis corresponds to the direction of the maximum moment of inertia. Realizing that the applied static field can be at any orientation with respect to this frame recasts the Zeeman interaction as $\mathcal{H}_z = \omega_x(t)J_x + \omega_y(t)J_y + \omega_z(t)J_z$

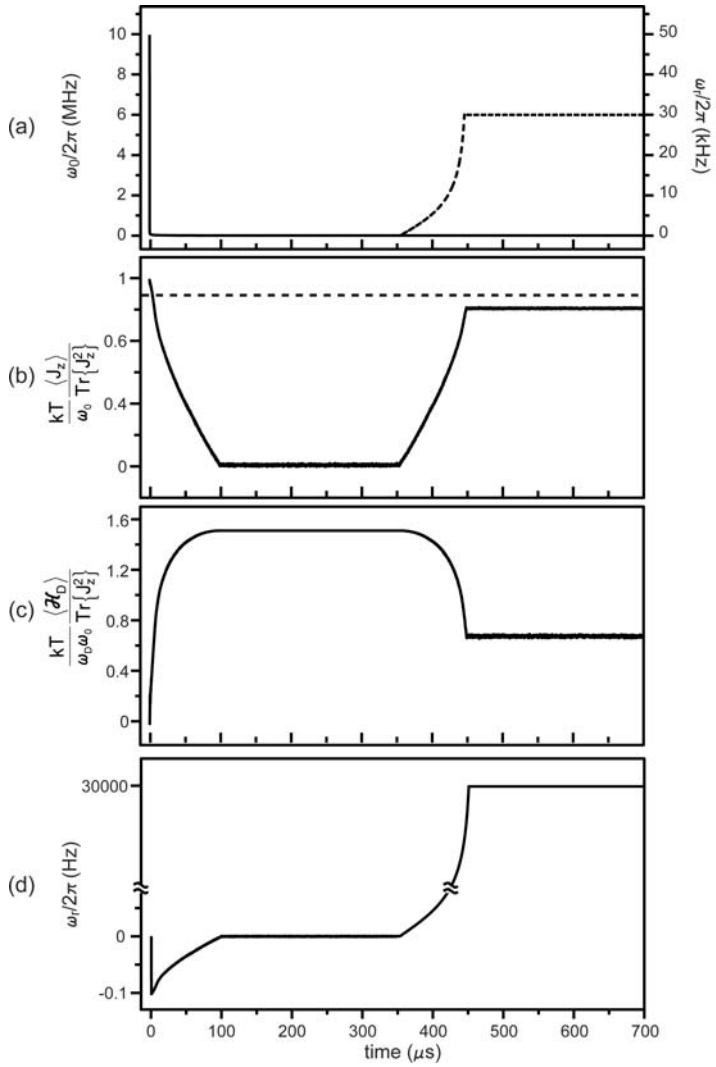

Fig. 5. Eight spin simulation of the effects of adiabatic demagnetization from a high $H_i = \omega_0/\gamma = 2,350\,\mathrm{G}$ magnetic field to zero field and subsequent remagnetization in an effective spinning field of $H_{ghost} = \omega_r/\gamma = 7.05\,\mathrm{G}$. The timing of the magnetic field and sample spinning is shown in (a) while the change in magnetization $\langle J_z\rangle$, dipolar order $\langle \mathcal{H}_D\rangle$, and sample spin rate ω_r are included in (b)–(d) respectively.

where it is understood that the J_x, J_y, and J_z operators pertain to the total spin angular momentum in the x, y, and z directions in the inertial frame while $\omega_x(t)$, $\omega_y(t)$, and $\omega_z(t)$ correspond to the time dependent orientation of the field $\boldsymbol{H} = \boldsymbol{\omega}(t)/\gamma = (\omega_x(t)/\gamma)\boldsymbol{i} + (\omega_y(t)/\gamma)\boldsymbol{j} + (\omega_z(t)/\gamma)\boldsymbol{k}$ in the inertia frame as the sample rotates. The three principal components of the inertia tensor I_{xx}, I_{yy}, and I_{zz} can be used along with the angular momentum conservation relation in (8) to develop a similar conservation rule for any general orientation of the DC field with respect to the sample rotation direction as

$$\frac{\mathrm{d}}{\mathrm{d}t}\begin{pmatrix} I_{xx}\omega_{r,x}(t) \\ I_{yy}\omega_{r,y}(t) \\ I_{zz}\omega_{r,z}(t) \end{pmatrix} = -\frac{\mathrm{d}}{\mathrm{d}t}\begin{pmatrix} \langle J_x\rangle \\ \langle J_y\rangle \\ \langle J_z\rangle \end{pmatrix} + \begin{pmatrix} 0 & -\omega'_z(t) & \omega'_y(t) \\ \omega'_z(t) & 0 & -\omega'_x(t) \\ -\omega'_y(t) & \omega'_x(t) & 0 \end{pmatrix} \begin{pmatrix} \langle J_x\rangle \\ \langle J_y\rangle \\ \langle J_z\rangle \end{pmatrix}, \tag{11}$$

where $\omega'_i(t) = \omega_i(t) + \omega_{r,i}(t)$, $i = x, y, z$ and $\omega_{r,i}(t)$ corresponds to the frequency of rotation of the object along the principal axes of I in the inertial frame. The expectation values of the total magnetization in (11) in the presence of a DC field are most easily obtained by expressing the Zeeman and homonuclear dipolar interactions in a rotating frame at the sample rotation frequency as

$$\begin{aligned} \mathcal{H}_{rot} = {} & (\omega_{r,x}(t) + \omega_x(t))\sum_{i=1}^{N} I_{x,i} + (\omega_{r,y}(t) + \omega_y(t))\sum_{i=1}^{N} I_{y,i} \\ & + (\omega_{r,z}(t) + \omega_z(t))\sum_{i=1}^{N} I_{z,i} + \sum_{i=1}^{N}\sum_{j\neq i}\omega_D(i,j)\sum(-1)^q T_q^{(2)}(I_i, I_j)R_{-q}^{(2)}(\theta_{i,j}, \phi_{i,j}), \end{aligned} \tag{12}$$

where the sum over all of the spins considered in the sample is included for clarity, $\omega_D(i,j) = \gamma_i\gamma_j\hbar/r_{i,j}^3$, and the polar angles $\theta_{i,j}$ and $\phi_{i,j}$ are included in the final term to specify that the internuclear direction $\boldsymbol{r}_{i,j}$ between each spin pair in the sample might have a different orientation with respect to the moment of inertia frame. In the special case of Barnett induced magnetization, the discussion in the previous sections suggests that any changes due to the feedback predicted in (11) in practical spin rates of several kHz along the $+z$ direction are small and most likely negligible. Taking $\omega_{r,x}(t) = \omega_{r,y}(t) \approx 0$ and $\omega_{r,z}(t) = \omega_r$ suggests that the only time dependence remaining in (12) in the rotating inertia frame is due to the precession of the applied DC field around the sample. The transverse $\omega_x(t)$ and $\omega_y(t)$ components will modulate at ω_r or equivalently, are at exact resonance with M_0 and will thus cause saturation transitions while the ω_z term is time independent and will add a detuning effect and thus a resonance offset. It is important to note that a similar effect occurs in standard magnetic resonance experiments when a DC field perpendicular to the Zeeman polarizing field is turned on in the lab frame. An initially polarized value of M_0 would disappear as it precesses

around the effective field at a rate depending on the size of the perpendicular field.

8 Lattice Structure Dependence of the Barnett Effect

In a liquid the dipole-dipole interaction between spins is cut off because of random fluctuations of the lattice coordinates. The competition between mutually interacting spins precessing in the local dipolar field and the apparent precession caused by a small ghost field H_{ghost} disappears if the local field averages to zero. To understand this averaging assume first that the dipolar coupling between two spins is zero. The two spins of course would precess about any applied DC field, but for the moment let them remain pointed in fixed directions in space like gyroscopes. One can easily see for example that rotation of the internuclear vector $\boldsymbol{r}$ by some precession angle about a perpendicular axis will alter the orientation angles of both dipoles relative to one another. Now turn on the dipole-dipole interaction. Comparison of the interaction energy at the two different orientations reveals that it is in fact different. If instead of two discrete angles a continuous set of angles is explored through sample rotation one finds that if the rotation rate ω_r is comparable to or exceeds the dipole-dipole coupling strength, the spins appear to be precessing coherently about the rotation axis perpendicular to $\boldsymbol{r}$ in the rotating frame. It is in this case that an apparent torque can be attributed to the fictitious field $H_{ghost} = \omega_r/\gamma$. As long as $\boldsymbol{r}$ retains the integrity of the lattice structure, the spins can sense Fourier components characteristic of the lattice rotation appearing in that frame and ultimately polarize by spin-lattice relaxation. But as stated above, if the lattice structure disappears because of coordinate fluctuations as in a liquid due to motional narrowing, the Barnett effect will be quenched. Basically the lattice environment becomes isotropic, looking virtually the same to the spins regardless of the rotational aspects of the liquid. If a torque is to be attributed to H_{ghost} in a rotating sample, the spins must mutually interact over many cycles of rotation in a reference frame that connects them to a fixed lattice structure.

9 Conclusion

One motivation for this work was the lure of polarizing nuclear spins in solids in conventional high field applications by transferring the massive angular momentum $I\omega_r$ from a rotating macroscopic object. The arguments provided in the above sections suggest that a small fraction of this massive sample angular momentum can indeed be transferred but only in low field situations where the sample rotation rate ω_r and Larmor frequency ω_0 is comparable to the dipolar coupling strength ω_D. At present conventional high field applications of this method to homonuclear dipole-dipole coupled spin systems are limited

because the high magnetic field quenches the spin-lattice coupling manifest in the non-secular dipole-dipole terms that drive the effect. Before identifying possible uses of the Barnett effect in nuclear spin systems, experiments must be completed to verify whether or not the ghost field does in fact behave like a real DC field. Instead of relying only on conservation laws to account for the transfer of angular momentum between the spin system and the rotor, the challenge remains to devise a more rigorous two reservoir formalism similar to that applied to cross relaxation between two spin species.

Acknowledgements

In particular, ELH is grateful to Dietmar Stehlik for stimulating discussions and initiating interest in the Einstein-de Haas and Barnett effects. We also gratefully acknowledge useful discussions with Alex Pines, Maurice Goldman, John Waugh, Jean Jeener, Eugene Commins, Carlos Meriles, Demitrius Sakellari, Andreas Trabesinger and Jamie Walls. MPA is a David and Lucile Packard and Alfred P. Sloan foundation fellow.

References

1. R. Mc Dermott, A.D. Trabesinger, M. Muck, E.L. Hahn, A. Pines, J. Clarke: Science **295**, 2247–2249 (2002)
2. D. Budker, D.F. Kimball, V.V. Yashchuk, M. Zolotorev: Phys. Rev. A **65**, 55403 (2002)
3. L.F. Bates: *Modern Magnetism* (University Press, Cambridge 1951)
4. (a) S.J. Barnett: Phys. Rev. **6**, 239–270 (1915)
   (b) S.J. Barnett: Rev. Mod. Phys. **7**, 129–166 (1935)
5. (a) A. Einstein, W.J. de Haas: Verhandl. Deut. Phsik. Ges. **17**, 152–170 (1915)
   (b) A. Einstein, W.J. de Haas: Verhandl. Deut. Phsik. Ges. **18**, 173–177 (1916)
6. J.H. Van Vleck: *The Theory of Electric and Magnetic Susceptibility* (Clarendon, Oxford 1932) pp 94–97
7. J.M.B. Kellogg, I.I. Rabi, N.F. Ramsey, J.R. Zacharias: Phys. Rev. **56**, 728–743 (1939)
8. (a) F. Bloch, W.W. Hansen, M. Packard: Phys. Rev. **70**, 474–485 (1946)
   (b) E.M. Purcell, H.C. Torrey, R.V. Pound: Phys. Rev. **69**, 37–38 (1946)
9. A. Abragam, B. Bleaney: *Electron Paramagnetic Resonance of Transition Ions* (Clarendon, Oxford 1970)
10. E.M. Purcell: Astrophys. J. **231**, 404–416 (1979)
11. A. Lazarian, B.T. Draine: Astrophys. J. **520**, L67–70 (1999)
12. D.K. Sodickson, J.H. Waugh: Phys. Rev. B **52**, 6467–6469 (1995)
13. B. Black, B. Majer, A. Pines: Chem. Phys. Lett. **201**, 550–554 (1993)
14. R.L. Strombotne, E.L. Hahn: Phys. Rev. **133**, A1616–A1629 (1964)
15. A. Abragam: *Principles of Nuclear Magnetism* (Clarendon, Oxford 1961)
16. M. Goldman: *Spin Temperature and Nuclear Magnetic Resonance in Solids* (Clarendon, Oxford 1970)